

## A FIRST MAP OF THE COSMIC MICROWAVE BACKGROUND AT 0.5 RESOLUTION

MARTIN WHITE AND EMORY F. BUNN

Center for Particle Astrophysics and Departments of Astronomy and Physics, University of California, Berkeley, CA 94720-7304

Received 1994 October 31; accepted 1995 February 1

## ABSTRACT

We use a maximum entropy technique to reconstruct a map of the microwave sky near the star  $\gamma$  Ursae Minoris, based on data from flights 2, 3, and 4 of the Millimeter-wave Anisotropy Experiment (MAX).

*Subject headings:* cosmic microwave background — methods: numerical

## 1. INTRODUCTION

The data from cosmic microwave background (CMB) anisotropy experiments is improving rapidly. The next generation of degree-scale experiments should have the capability to map significant regions of the sky. However, owing to uneven sky coverage, differencing strategies, and noise in the data, reconstructing a temperature map from the observations will be nontrivial. It is therefore of interest to begin developing techniques for this task.

The Millimeter-wave Anisotropy Experiment (MAX) has now accumulated data on the temperature anisotropies in the CMB near the star  $\gamma$  Ursae Minoris ( $\gamma$  UMi) from three separate flights (Alsop et al. 1992; Meinhold et al. 1993; Devlin et al. 1994). This data covers  $\sim 10^\circ \times 5^\circ$  on the sky, with the central  $5^\circ \times 2^\circ$  being densely sampled (see Fig. 1), and thus is ideal for testing algorithms for constructing maps of the microwave sky.

In studies of CMB anisotropies it has been common to assume that the fluctuations are Gaussian distributed and that the overall phases of the anisotropy in our universe are irrelevant. In this paper we would like to consider an alternative approach, in which maps of the microwave sky in particular regions are made. As an example of the method, we concentrate on the region of sky near  $\gamma$  UMi where a large data set already exists. The advantage of making CMB maps, apart from the simple desire to map the whole sky in as many wavebands as possible, is that it allows us to develop a catalog of features for comparison with other experiments. In addition, one can look for properties of the sky which are not predicted by theories and could be overlooked in statistical analyses. While detailed comparison of observations of the same region of the sky by different experiments should be done by statistical comparison of the raw data sets (e.g., cross-correlation of the temperature difference maps in current experiments), having a map of the sky in the region of interest is helpful in planning flights and obtaining a visual representation of the region to be surveyed. Additionally, these maps can be used to correlate phase information through the method of constrained realizations (e.g., Hoffman & Ribak 1991; Bunn et al. 1994), which can allow predictions to be made for other experiments.

Any inversion procedure of this kind, where we attempt to reconstruct a temperature map from a small region of the sky where only temperature differences are measured, requires a regularization procedure. For example, to construct a map one needs information on the long-wavelength contributions which are not well constrained by the data set. In this paper we shall adopt the *maximum entropy* procedure (MaxEnt), often used in

other branches of astronomy (see below). MaxEnt provides a method for choosing among the many maps which could lead to the observed data. The advantage of this method for our purposes is that it reconstructs the “smoothest” maps consistent with the data. If it is our intent to search for features in the maps, such as hot or cold spots or indications of non-Gaussian structures (such as lines), this is clearly the most conservative regularization. Whenever the inversion is not unique a choice needs to be made, and we take the stance that we wish to introduce only those features which are *required* by the data, even if this can miss features which are *allowed* by the data.

In the past, Wiener filtering has often been employed for this purpose (Bunn et al. 1994; Fisher et al. 1994; Lahav et al. 1994; Zaroubi et al. 1994). This procedure requires additional assumptions beyond those required for MaxEnt, and can in principle be more powerful. In particular, Wiener filtering requires the assumption of a particular power spectrum and distribution of fluctuations. (In principle, the power spectrum can be estimated from the data set itself. This is usually possible for a data set with high signal-to-noise ratio and many correlated pixel pairs; it is not feasible with the MAX data.) Since our goal in this paper is to present a method for identifying robust features in a model-independent way, we have chosen to use MaxEnt rather than Wiener filtering. Our purpose is to reconstruct a map of the observed sky with as few assumptions as possible.

## 2. MAXIMUM ENTROPY METHOD

The main use of the maximum entropy method is to provide a regularized inversion procedure for noisy and incomplete data. In practice, what one does is construct a model, which in our case consists of the temperature values in  $N_{\text{pix}} = 64 \times 64$  pixels on a  $30^\circ \times 8^\circ$  patch of the sky. We attempt to find the best model sky given data  $T_k \pm \sigma_k$  at some locations  $\hat{n}_k$  with  $k = 1 \cdots N_{\text{obs}}$ . We assume the errors,  $\sigma_k$ , are Gaussian and independent. In the MaxEnt method we minimize not the  $\chi^2$  associated with the fit of this “theory” to the data, but rather the combination

$$S + \lambda \chi^2, \quad (1)$$

where the entropy  $S$  will be discussed in detail below and  $\lambda$  is a Lagrange multiplier which determines the relative weight given to the two terms. The first term ( $S$ ) will be extremized when the map is as featureless as possible, while the second tries to make the model temperature values agree with the data as closely as possible. Maximizing the combination should lead to the smoothest map consistent with the data and has the advantage of being computationally simple. Our result will be the most

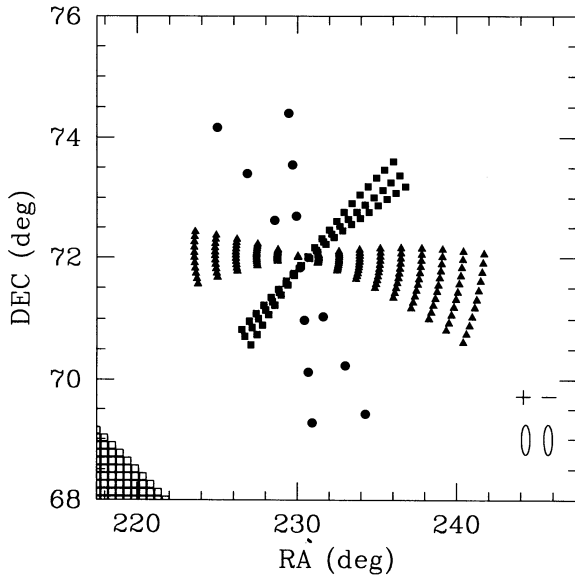


FIG. 1.—The region of sky, near  $\gamma$  UMi, covered by the second, third, and fourth flights of the MAX experiment. The solid circles represent data from the second flight, triangles those from the third, and squares those from the fourth. For reference, we show the beam pattern as the two circles (labeled *plus* and *minus*) for the MAX differencing strategy in the lower right. The apparent elliptical shape is due to the axis ranges chosen for the plot. Also shown (lower left) is the size of the pixels used in the map.

conservative picture of deviations from uniformity consistent with the data.

There is a large body of literature on the MaxEnt method. For information on its use in an astronomical context see, e.g., Gull & Daniell (1978), Burch, Gull, & Skilling (1983), Cornwell & Evans (1984), Narayan & Nityananda (1986), Lahav & Gull (1989), Skilling (1991), Press et al. (1992), or the proceedings of the several MaxEnt workshops and conferences (and the references therein).

Traditionally, when dealing with intensity maps, one takes the entropy function to be  $S = -I \log I$ , which requires  $I \geq 0$ . In our case the analogous procedure would be to use as our model the absolute temperature on the sky (obtained by requiring the data to have an average temperature of 2.726 K, for example). However, since the temperature fluctuations in the data are 1 part in  $10^5$  this can lead to numerical problems. Using simply the temperature differences as our model (i.e., subtracting a mean  $T$  from each point) leads to problems with the evaluation of the logarithm in  $S$ . Note, however, that the role of the entropy function is to “smooth” the inversion. The overall offset and range of the pixel values in the model is not relevant to this question. We can say mathematically that the extremum of the entropy is invariant under rescalings and shifts of the origin, so we rescale the temperatures before computing the logarithm.

There are other definitions of the entropy which can be used (see Narayan & Nityananda 1986 for a discussion). In the context of Bayesian inference, a choice of  $S$  corresponds to a choice of prior information, and the inferences should be robust under changes in “prior.” We shall stick with the  $I \log I$  definition since it enforces “smooth” maps.

This leads us to consider the relative weight assigned to the entropy and the  $\chi^2$ , which is given by  $\lambda$ . Often one assigns to  $\lambda$  the value required so that the  $\chi^2$  of the best-fit model is approximately equal to the number of data points. (In this case,  $\lambda$  is a Lagrange multiplier introduced to enforce the  $\chi^2$  constraint

while maximizing the entropy.) This can be implemented straightforwardly during the solution of the MaxEnt inversion. Alternatively (Gull 1989; Lahav & Gull 1989), one can use the eigenvalues of the Hessian matrix, which is less arbitrary since it can be justified from Bayesian considerations. Generally, the resulting map is independent of the choice of  $\lambda$  over a large range, and hence we will stick with the former prescription even though it has an element of arbitrariness.

Having fixed  $\lambda$ , one proceeds to solve the data by an iterative method. A more generic and powerful alternative is a maximum search algorithm (Burch et al. 1983; Cornwell & Evans 1985); however, we have found the iterative solution to converge stably and rapidly to the desired solution, obviating the need for complicated strategies. Let us call  $t_j$  the temperature values in our “model” map, where  $j$  runs from 1 to  $N_{\text{pix}}$ . Let  $B_{k,j}$  be the beam profile function which acts on the model pixels and predicts the measured temperature differences  $\tau_k = \sum_j t_j B_{k,j}$  ( $k = 1 \cdots N_{\text{obs}}$ ). One now starts with a uniform map and iterates the equation (Gull & Daniell 1978)

$$t_j = \exp \left( -\text{const}_1 + \lambda \sum_{k=1}^{N_{\text{obs}}} B_{k,j} \frac{T_k - \tau_k}{\sigma_k^2} \right) + \text{const}_2, \quad (2)$$

where recall  $T_k \pm \sigma_k$  are the temperature differences to be fitted. This equation comes from extremizing equation (1) with respect to the  $t_j$ , and the values of the constants specify the zero and range of the temperature scale. We have chosen these constants so that unmeasured parts of the map are assigned zero temperature offset.

### 3. MAX DATA SET

The MAX experiment is a subdegree scale CMB anisotropy experiment which measures temperature differences on the sky over a range of frequencies. In the following we shall assume that all of the signal seen in the  $\gamma$  UMi scan is purely that of CMB anisotropies, so we co-add all the frequency channels to increase the signal-to-noise ratio. If this turns out not to be the case, the method could also be implemented for each frequency separately.

The temperature “differences” are defined by performing a sinusoidal chop, at a frequency of  $\nu = 6$  Hz, with amplitude  $\alpha_0 = 0.65$  parallel to the scan direction of the telescope. The signal is demodulated at the first harmonic of the chop frequency so that the temperature assigned to the point  $\hat{n}$  is

$$\tilde{T}(\hat{n}) \equiv -3.34 \int_0^{1/\nu} dt \nu \sin(2\pi\nu t) \Theta[\hat{n} \cos \alpha(t) + \hat{i} \sin \alpha(t)], \quad (3)$$

where  $\alpha(t) = \alpha_0 \sin(2\pi\nu t)$ ,  $\hat{i}$  is a unit vector lying along the chop direction and perpendicular to  $\hat{n}$ , and  $\Theta(\hat{n})$  is the beam-smoothed temperature at  $\hat{n}$ . See Srednicki et al. (1993) for more details. To obtain an effective beam profile we replace  $\Theta$  in the above with the beam weight function, which we take to be a Gaussian of width  $0.5$  FWHM. The beam width varied slightly from flight to flight, which we have included in the analysis.

The data available from the MAX group has had an offset subtracted from each “scan.” This has the effect of modifying the long-wavelength modes reconstructed by our procedure. Since these modes are not well constrained by the data in any case, we have not tried to correct for this effect.

### 4. RESULTS AND CONCLUSIONS

We show in Figure 2a our estimated map, which is consistent (by construction) with the three MAX- $\gamma$  UMi data sets.

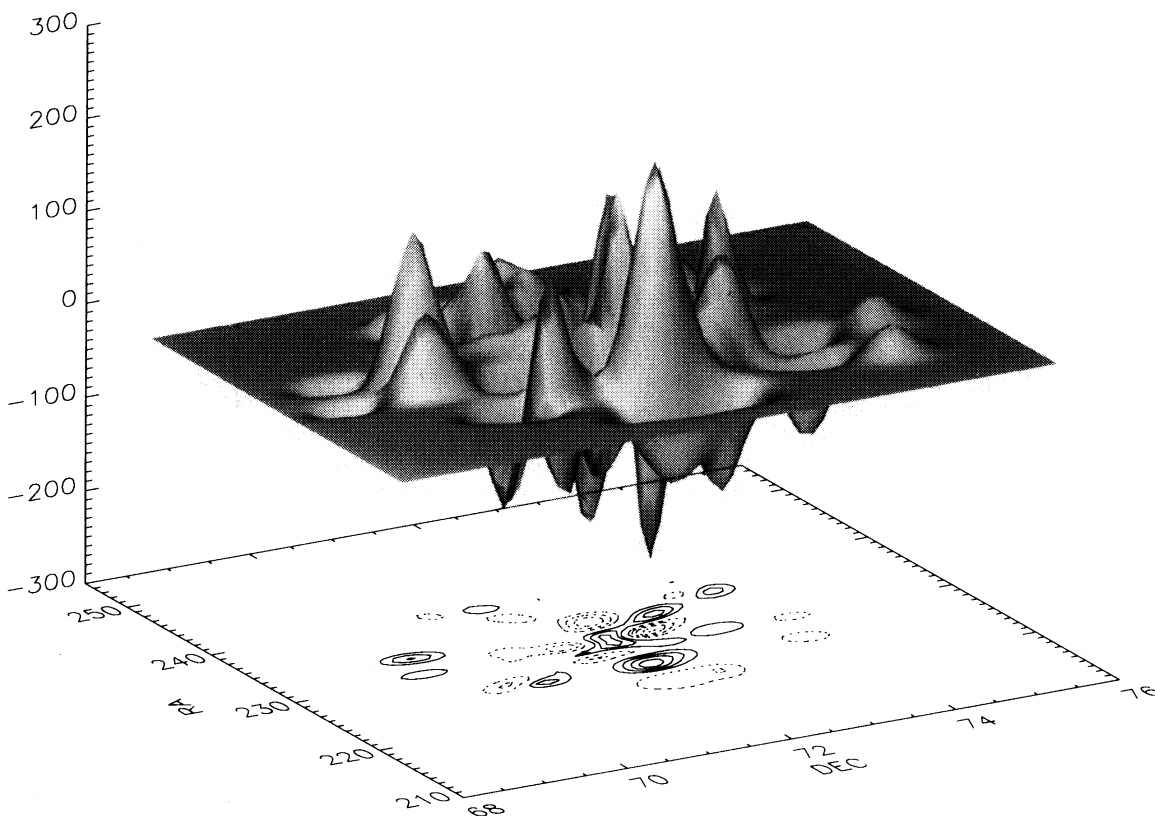


FIG. 2a

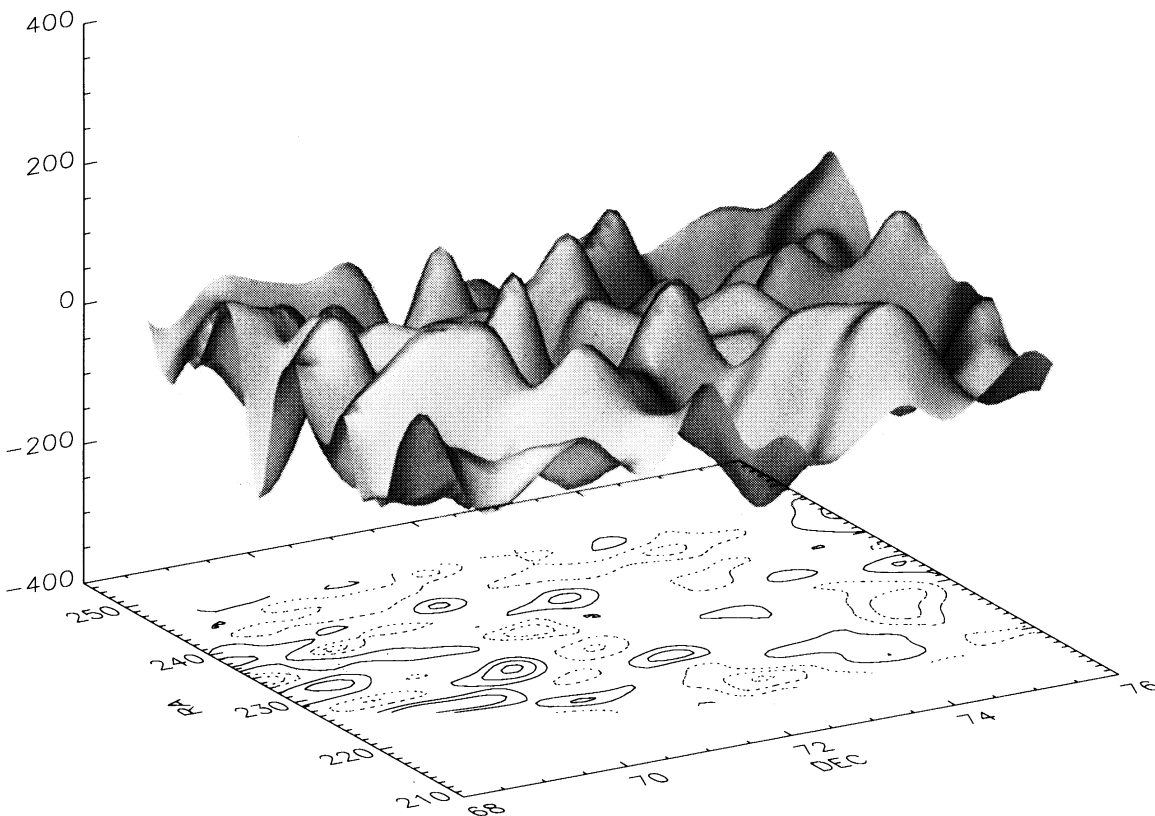


FIG. 2b

FIG. 2.—(a) The reconstructed sky temperature, in  $\mu\text{K}$ . Since the MAX experiment measures only temperature differences, the “zero” of the temperature scale is arbitrary. The contours are spaced at intervals of  $50 \mu\text{K}$ . (b) A sky simulated using a cold dark matter model normalized to COBE and with  $\Omega_0 = 1$ ,  $H_0 = 50 \text{ km s}^{-1} \text{ Mpc}^{-1}$ , and  $\Omega_b = 0.05$ , smoothed on  $0.5^\circ$  and with power on wavelengths larger than the box removed.

The pixels are distributed exponentially in temperature, presumably reflecting our assumption of Gaussian beams. The rms of the nonzero portions of the map is consistent with the expected fluctuations in a model such as cold dark matter (CDM). In Figure 2*b* we show a realization of a standard CDM sky, smoothed on  $0\text{.}5$  and with power on wavelengths larger than the box removed. The maps are qualitatively similar, though there is a large degree of arbitrariness in statistical comparison which makes it difficult to compare quantitatively. Our map appears to have more small-scale structure and less large-scale structure than the CDM map, possibly reflecting that our procedure reconstructs small-scale power better than large scale power. This is not unexpected given the small amount of sky ( $\sim 25$  square degrees) for which we have data.

To test the accuracy of our reconstruction, we have simulated a MAX data set using our standard CDM model and used the same algorithm to reconstruct a map based on this synthetic data set. The resulting map (not shown) is very similar to Figure 2*a*, having an exponential pixel distribution and more small-scale power than Figure 2*b*. The reconstructed map is quite successful at locating actual features in the simula-

tion. Of the 10 largest extrema in the reconstructed map, eight correspond closely to strong peaks of the same sign in the original simulation. (The separations between the true peaks and the recovered peaks are  $\sim 0\text{.}5$ , consistent with our expected resolution.) The two "failures" both lie on the outer edges of the MAX-3 region where the signal-to-noise ratio is relatively low. A more detailed study of the biases in this reconstruction method still remains to be done.

In conclusion, we have presented a method for constructing temperature maps of the CMB which can be easily applied to differencing experiments which cover only a small fraction of the sky. As an application of this method, we have constructed the "most likely" picture of the microwave sky consistent with the data in the region near  $\gamma$  UMi. While comparison of scans and model testing should be done statistically using the differenced data, this method allows one to check for features which are contrary to expectations and to plan future observations.

We would like to thank Douglas Scott and Joseph Silk for useful conversations and encouragement, and Mark Devlin and Stacy Tanaka for help with the MAX data.

#### REFERENCES

- Alsop, D. C., et al. 1992, *ApJ*, 395, 317  
 Bunn, E. F., et al. 1994, *ApJ*, 432, L75  
 Burch, S. F., Gull, S. F., & Skilling, J. 1983, *Comput. Vision, Graphics, & Image Processing*, 23, 113  
 Cornwell, T. J., & Evans, K. F. 1985, *A&A*, 143, 77  
 Devlin, M., et al. 1994, *ApJ*, 430, L1  
 Fisher, K., et al. 1994, *MNRAS*, submitted  
 Gull, S. F. 1989, in *Maximum Entropy and Bayesian Methods*, ed. J. Skilling (Dordrecht: Kluwer)  
 Gull, S. F., & Daniell, G. J. 1978, *Nature*, 272, 686  
 Hoffman, Y., & Ribak, E. 1991, *ApJ*, 380, L5  
 Lahav, O., & Gull, S. F. 1989, *MNRAS*, 240, 753  
 Lahav, O., et al. 1994, *ApJ*, 423, L93  
 Meinhold, P. F., et al. 1993, *ApJ*, 409, L1  
 Narayan, R., & Nityananda, R. 1986, *ARA&A*, 24, 127  
 Press, W. H., et al. 1992, *Numerical Recipes*, 2d ed. (Cambridge: Cambridge Univ. Press)  
 Skilling, J. 1991, *Nature*, 353, 707  
 Srednicki, M., White, M., Scott, D., & Bunn, E. 1993, *Phys. Rev. Lett.*, 71, 3747  
 Zaroubi, S., et al. 1994, *ApJ*, submitted